Microfluid Nanofluid (2016) 20:135
DOI 10.1007/s10404-016-1800-8

RESEARCH PAPER

Precise capillary flow for paper-based viscometry

Emanuel Elizalde[1] · Raúl Urteaga[1] · Claudio L. A. Berli[2]

Received: 11 May 2016 / Accepted: 3 September 2016

Abstract The imbibition dynamics of aqueous solutions in paper substrates determines the performance of all the operations integrated in analytical paper-based devices. In particular, an accurate control of the flow rate is required for quantitative analysis such as viscometry. This work experimentally investigates paper filling dynamics in order to find a strategy to improve the precision and predictability of the imbibition process. The effect of performing successive wetting–drying cycles on the same strips is explored, since we have discovered that, after around four cycles, the filling kinematics is highly repetitive, and data closely follow the theoretical Lucas–Washburn model. It is found that the cyclic process enables quantitative assessment of the filling dynamics with uncertainties lower than 0.8 %. Implementing this protocol, paper-based viscometry with a precision around 1 % was experimentally demonstrated. This knowledge is of interest to develop paper-based microfluidic devices with a new level of precision.

Keywords Paper-based microfluidics · Capillary filling · Viscometry

1 Introduction

Microfluidic paper-based analytical devices (μPADs) are a new class of point-of-care diagnostic devices that are inexpensive, easy to use, and specifically designed for applications in developing countries (Martinez et al. 2010; Cate et al. 2015). While qualitative μPADs assays are widely used in the form of dipsticks and lateral flow tests, quantitative tests still suffer from certain limitations such as the lack accuracy and sensitivity. The capillary filling of paper with aqueous solutions (sample, reagents, diluents, etc.) is the fundamental phenomena behind the transport of analyte and chemical species in paper-based devices. An accurate control of the flow rate would lead to a better handling of time-dependent operations like sequential mixing, kinetic reactions, and DNA amplification, which are being integrated on paper-based devices with a constantly growing level of sophistication (see for instance Connelly et al. 2015). It is noteworthy that the variability of fluid velocity particularly affects the precision of devices using distance-based or time-based readout (Noh and Phillips 2010a, b; Lewis et al. 2013; Cate et al. 2013; Songok and Toivakka 2016; Jahanshahi-Anbuhi et al. 2014). In particular, given the well-known linear relationship between the viscosity of Newtonian fluid and filling time, one can perform paper-based viscometry simply measuring imbibition time (Li et al. 2014). The precision of viscosity measurement is then limited by the dispersion of imbibition time. Furthermore, it has been recently shown that non-Newtonian fluids produce specific changes in the kinematics of capillary imbibition (Berli and Urteaga 2014; Shou and Fan 2015). High-precision experimental setups are thus required to develop paper-based rheometers able to measure subtle deviations from Newtonian behavior. Therefore, detailed studies of capillary imbibitions on paper substrates are necessary to

Electronic supplementary material The online version of this article (doi:10.1007/s10404-016-1800-8) contains supplementary material, which is available to authorized users.

✉ Claudio L. A. Berli
cberli@santafe-conicet.gov.ar

[1] IFIS-Litoral, UNL-CONICET, Santa Fe, Argentina

[2] INTEC, UNL-CONICET, Santa Fe, Argentina

Published online: 14 September 2016

improve the analytical performance of μPADs, as well as to find new designs and capabilities (Martinez et al. 2010).

In recent works, the imbibition dynamics has been satisfactorily described by using a continuous media approach and an effective permeability coefficient (Xiao et al. 2012; Wang et al. 2013; Shou et al. 2014; Joung et al. 2014; Elizalde et al. 2015). In particular, for uniform strips, theoretical predictions coincide with the classical Lucas–Washburn model (Lucas 1918; Washburn 1921), which indicates that the distance l penetrated by the liquid as a function of time t should satisfy

$$l = \sqrt{dt} \tag{1}$$

where d is a sort of diffusive coefficient that characterizes the substrate–fluid system. In particular, d is inversely proportional to the fluid viscosity (Elizalde et al. 2015). Most of research works on the subject make use of Eq. 1 to characterize paper substrates and meter flow rates (Yetisen et al. 2013). However, the variability found in the experimental values of the coefficient d is too large to be associated with inaccuracies in geometrical dimensions or macroscopic shapes (Bohm et al. 2014; Liu et al. 2015; Elizalde et al. 2015). In fact, deviations from Eq. 1 are usually reported, and corrections have been also proposed considering paper swelling (Masoodi and Pillai 2010), evaporation (Songok et al. 2014), the fractal character of porous media (Cai et al. 2010), and the effect of wax boundaries (Hong and Kim 2015). The central problem for our work is that the dynamics of capillary imbibition of paper substrates has an inherent statistical variation, since fluid velocity depends on the particular way in which constituent cellulose fibers are arranged (Alava et al. 2004). This variability is a characteristic of the medium and therefore uncontrollable once the paper has been produced. Also concerning industrial papers, it is well known in pulp and paper science (Alava et al. 2004) that cellulose fibers are slightly oriented in the called machine direction (MD). The transversal direction is called cross direction (CD). As fiber orientation influences the liquid penetration in the structure, an anisotropic permeability is generated in the production process: the fastest capillary flow results in the MD and the slowest in the CD. One may readily infer that taking into account this directionality improves the predictability of the imbibition dynamics. Nevertheless this issue is often overlooked or not properly discussed in the μPADs literature, which results in a considerable source of dispersion in reported data.

In the following, we introduce further aspects regarding the uncertainties of capillary filling in paper strips. Considering the distance reached by the fluid front at a given time, the overall dispersion reported in literature is about 10 % (Liu et al. 2015; Elizalde et al. 2015; Bohm et al. 2014; Noh and Phillips 2010b). Under these conditions, a paper-based viscometer is limited to 10 % precision. In addition, according to Eq. 1, plotting the squared position as a function of time should generate straight lines. However, experimental curves show a slight bending which is normally overlooked. Although deviations from the theoretical prediction may appear subtle, they are crucial for quantitative measurements such as those needed in paper-based rheometry. In fact, a power law fluid should produce an imbibition dynamics with $l \propto t^{\frac{n}{n+1}}$ where n is the flow behavior index of the fluid (Berli and Urteaga 2014; Shou and Fan 2015). Therefore, the accurate determination of this exponent (to characterize the non-Newtonian behavior of a liquid sample) is limited by these uncertainties.

In this context, the aim of the present work is to experimentally investigate the imbibition dynamics in paper strips, in order to find a strategy to improve the precision and predictability of the filling process. In particular, we explore the effects of performing successive wetting and drying cycles on the same strips, since we have figured out that this procedure leads to the following simultaneous behaviors: The imbibition dynamics becomes highly repetitive, and data fit precisely to Lucas–Washburn model Eq. 1. On the basis of these results, we develop a paper-based viscometer with a precision around 1 %. Measuring fluid viscosity on a paper-based device embodies all the advantages of microfluidics: small size, portability, low cost, power free, integrability, and low sample volume consumption.

2 Materials and methods

2.1 Materials

Whatman chromatographic paper (grade 3mm Chr, $46 \times 57\, cm^2$ sheets) and Whatman filter paper (grade 1, 120 mm disks) were used in experiments. Highly hydrophobic double-sided adhesive tape (Stiko, Silkstone SA, Buenos Aires, Argentina) was used to fix the paper strips. Deionized water was produced by using an inverse osmosis purifier (Osmoion, Apema SRL, Villa Domínico Argentina). High-quality sucrose (Refineria San Martin del Tabacal, Salta Argentina) and anhydrous glycerol (Cicarelli, Reagents SA, San Lorenzo, Argentina) were used for viscosity measurement.

2.2 Identification of fast and slow flow directions

A series of simple experiments were designed to detect MD and CD over paper samples. Figure 1a shows a paper sample over a beaker. A little drop of water was placed in the center of the paper sheet. The liquid radially infiltrates the paper forming an ellipse. The large axis of this ellipse indicates MD (blue line) and the shorter one indicates the CD (red line). The free paper in Fig. 1a curls because of

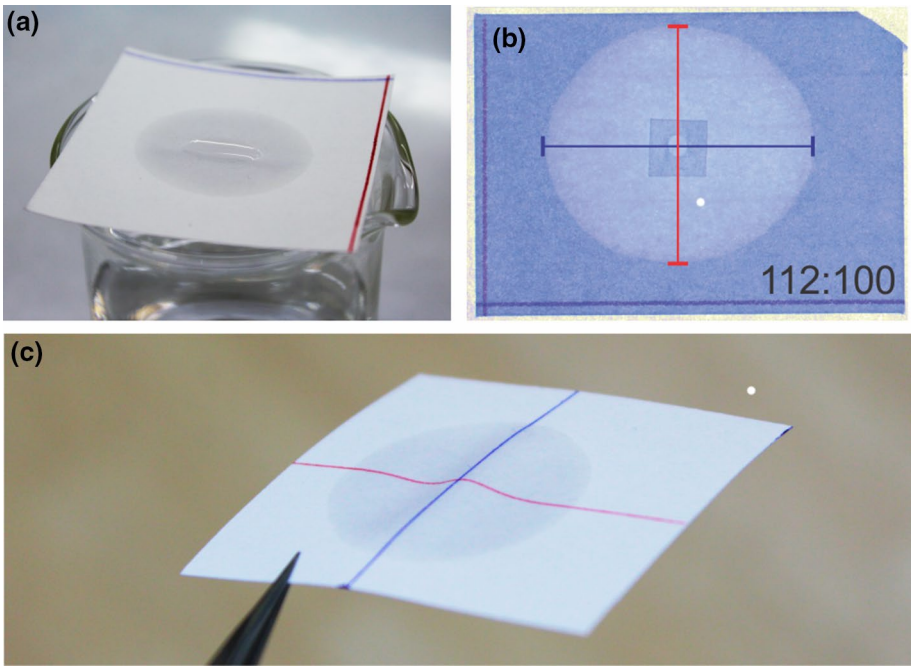

Fig. 1 Experiments made to identify paper directionality. **a** Chromatography paper sample holds free over a beaker. The liquid front due to the infiltration of a water drop forms an ellipse. **b** Radial imbibition in a paper sample fixed with hydrophobic tape forms an ellipse too. **c** Same as in (**a**), where *two lines* were marked to improve the visualization of paper curling. In all pictures, *blue lines* indicate the fast flow direction (MD) and *red lines* indicate the slow one (CD) (color figure online)

anisotropic swelling, forming a visible depression. Figure 1b shows the radial imbibition in a paper sample fixed over double-sided tape to avoid expansion and curling. As the ellipse still forms, Fig. 1b demonstrates that the existence of directionality is not a consequence of paper curling but an effect associated with cellulose fibers arrangement. Finally, Fig. 1c presents another paper sample with previously marked directions. This picture shows that the paper expansion after wetting is bigger in CD, as evidenced by the red line curling.

2.3 Paper-based device

Once main flow directions have been identified, a cutting template was fixed to the paper. This template is made of normal office paper with printed cutting marks. A second layer of office paper was put under the sample. In order to define strip boundaries, the sandwich was cut by using a sharp cutter and a ruler over a glass surface. The extra paper layer protects the paper sample against ripping. Following this procedure, paper strips of $5 \times 55\,\text{mm}^2$ were obtained.

The details of the fabricated device are schematically presented in Fig. 2a. A piece of hydrophobic double-sided tape was placed over a supporting glass. Chromatography paper strips were fixed over this double-sided tape. A little piece of double-sided tape was placed near one strip end (top left in the figure). This piece forms a hydrophobic barrier and delimits an inlet area of $5 \times 5\,\text{mm}^2$. The hydrophobic barrier prevents liquid creeping over the strips, so that the liquid infiltrates laterally only. The hydrophobic barrier allows us to define the initial position with high accuracy ($350\,\mu\text{m}$). The total length available for capillary filling is 50 mm and the filling time is approximately 10 min. Imbibition starts when a water drop is laid in the inlet area. A glass slide covers the strips with an air gap of about 1 mm to minimize evaporation.

2.4 Experimental setup

Capillary filling dynamics was followed by using a digital camera (Canon EOS Rebel T5). The devices were horizontally placed over a backlighting LED panel (LED light minimizes thermal effects). This setup avoids the use of dyes, taking advantage of translucent property of wet paper (Fig. 2b). The camera was focused vertically at a distance around 20 cm, connected to a PC. The spatial resolution was 36μ m and the time resolution was 12 frames per minute. In order to minimize uncertainties in the initial time, the drop was released in the inlet area immediately after triggering the first picture (within 1 s).

2.5 Image analysis

A typical picture sequence of a paper strip during imbibition is shown in Fig. 2c. A script was implemented to automatically analyze the images and extract the position l as a function of t. The procedure involves subtraction of the first image to each image and then normalization by the last one. The resulting matrix is laterally averaged, thus obtaining a longitudinal saturation profile. A cutoff level of 10 % was imposed to determine the mean liquid front position. A variation of

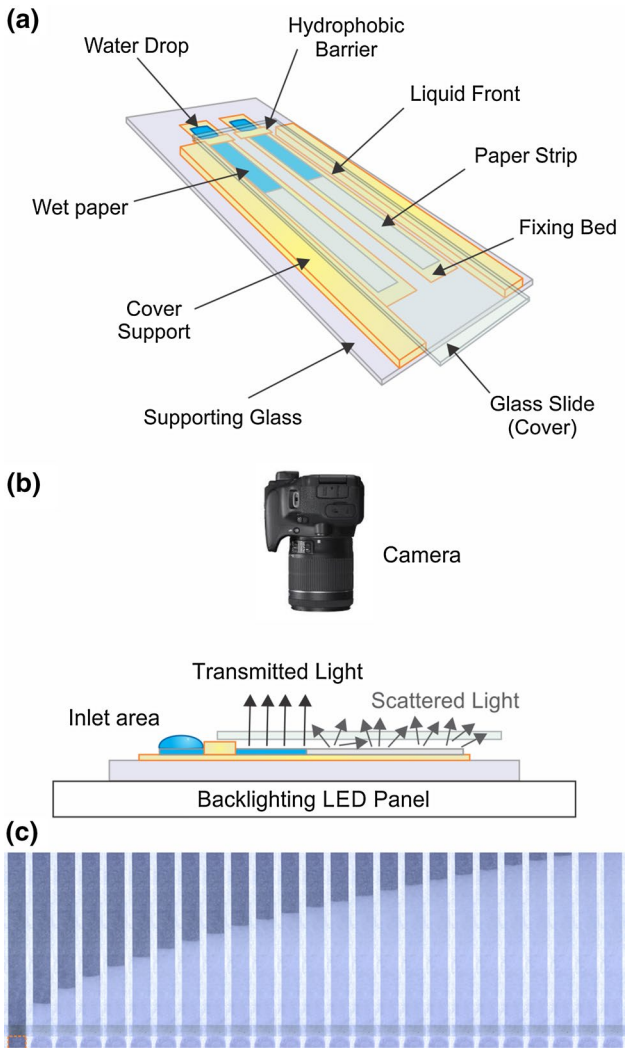

Fig. 2 **a** Paper-based devices consist of paper strips fixed over a glass by hydrophobic double-sided tape. Water is supplied trough the inlet located at one strip end (*top left*). **b** Experimental setup for imbibition experiments. The liquid front position was recorded by using a high-resolution digital camera. The microfluidic device was placed horizontally over a LED backlight panel. **c** Typical image sequence obtained during an experimental run with chromatography paper. Wet paper appears brighter in the pictures, providing a good definition of the imbibitions front. The interval between consecutive pictures is 30 s. The water drop and the hydrophobic barrier can be observed at the *bottom* of the picture. The inlet area is highlighted in the first frame

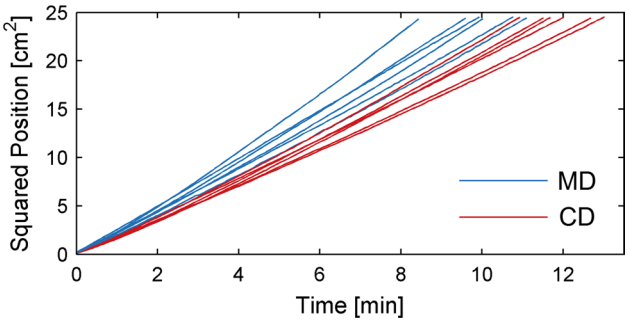

Fig. 3 Squared position as a function of time for capillary filling of 12 chromatography paper strips. Strips were cut following the machine (*blue*) and cross (*red*) direction (color figure online)

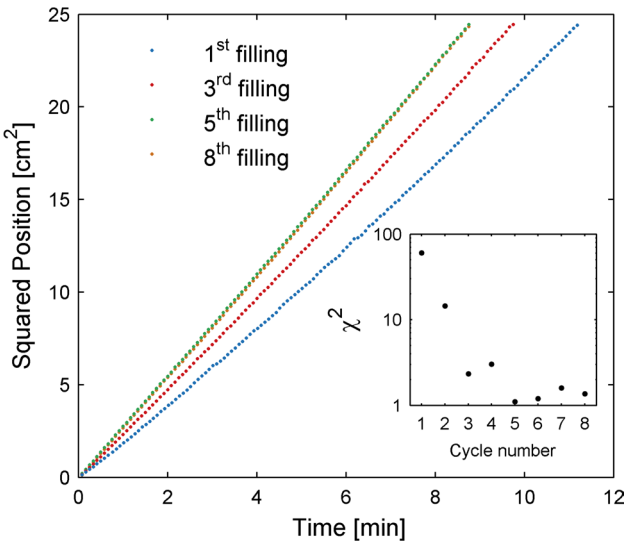

Fig. 4 Squared position as a function of time for the imbibition of a typical strip. Colors identify different cycles: 1st (*void blue*), 3rd (*red*), 5th (*green*), and 8th (*orange*). The *insets* present the reduced χ^2 for data fitting to Lucas–Washburn model (color figure online)

only 100 μm is derived from the selection of this cutoff value (see supplementary material for additional details). One filling curve (l and t vectors of approximately 120 data points) is obtained for every cycle (8) performed on each strip (6).

2.6 Wetting–drying cycles

The experimental setup allows one to repeat the capillary filling experiment over the same paper sample. After full wetting, the paper-based device was dried in a oven (20 min, 90 °C) and then cooled at room temperature during 20 min. In each wetting–drying cycle, the paper strips were subjected to identical conditions. The process was repeated eight times.

3 Results and discussion

Results shown throughout this section were obtained with chromatography paper; analogous experiments were carried out on filter paper, and results are reported in the supplementary material. First of all, we revise the basic aspects regarding the uncertainties of capillary filling in paper strips by using a practical example. Figure 3 presents squared position vs. time curves (where the expected response is a

straight line when Eq. 1 is satisfied) for the imbibitions of 12 chromatography paper strips of uniform width. Strips were cut taking into consideration the two principal directions of the paper sheet, i.e., MD (blue curves) and CD (red curves). The experimental data shown in Fig. 3 reveal three main features: First, it is effectively observed that blue and red curves form groups with differentiated slopes, meaning well-differentiated imbibitions velocities. Second, considering the distance reached by the fluid front at a given time, the overall dispersion among different tests in Fig. 3 is about 7 % (root mean square deviation). If one independently considers the slow and fast directions, the dispersions are only 3 and 5 %, respectively. Third, experimental curves slightly depart from Eq. 1 as mentioned in introduction. The effect becomes evident in cases where the curves cross each other. This aspect will be discussed in detail below.

3.1 Wetting–drying cycles

The effects of wetting–drying cycles were studied by using the fabricated devices. Figure 4 presents data of the squared position of the liquid front as a function of time for a typical paper strip. Only cycles 1, 3, 5, and 8 are presented for the sake of clarity. The figure shows the evolution of filling dynamics along the cycles, where two main phenomena occur. In first place, as the number of cycles increases, the data are more consistent with Lucas–Washburn model, i.e., the curves become more straight. In second place, the filling kinematics becomes repetitive, to the point that data from 5th and 8th cycles closely overlap (green and orange circles, respectively). It is relevant to point out that none of these phenomena occur in experiments where the paper strips are not fixed to a rigid substrate. Additional experiments were carried out, in which the material was heated (20 min at 90 °C) prior to the first wetting. No statistical difference on the filling dynamics was found (see supplementary material for details).

Experimental curves were fitted to Eq. 1, taken as the theoretical reference. To evaluate the goodness of fit (Press et al. 2007), the reduced Chi-square (χ^2) was calculated for each cycle and the results are shown in the inset of Fig. 4. One can observe that this value, which is a measure of fitting goodness, dramatically decreases from about 60 for the first cycle to around 1 for the fifth and higher cycles. Therefore, although discrepancies with Lucas–Washburn model seem small on a visual inspection, they have statistical significance. It is worth to remark here that the experimental setup, together with the image analysis procedure, allows one to achieve high precision in determining the imbibition front position (100 μm).

In order to better rationalize deviations from $\sqrt{t}$ dynamics (Eq. 1), all the experimental curves were fitted to a power law function of the form

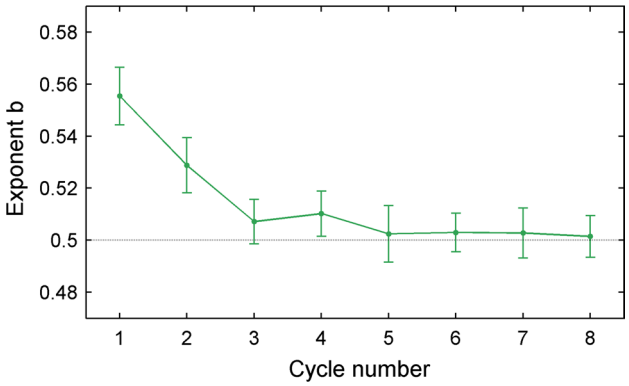

Fig. 5 Exponent of the power law function (Eq. 2) for different subsequent cycles. Dots represent the mean value for six strips and *bars* represent the standard deviation. The *dashed line* indicates the value predicted by Lucas–Washburn model

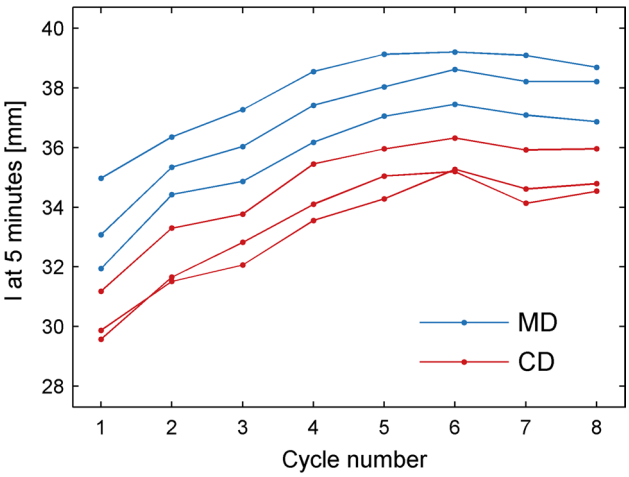

Fig. 6 Position of the liquid front l at 5 min, for subsequent cycles performed on six different strips. *Colors* identify fast (*blue*) and slow (*red*) flow directions (color figure online)

$$l = at^b \tag{2}$$

where a and b are the fitting parameters. Equation 2 coincides with Lucas–Washburn model when $b = 0.5$ and $a = \sqrt{d}$.

Figure 5 presents the power index b obtained for each cycle. Dots are the mean value for six devices (3 in MD and 3 in CD), and the bars represent the corresponding standard deviation. It is observed how the exponent evolves with the cycles toward Lucas–Washburn prediction, that is $b = 0.5$ (dashed line in Fig. 5). A convergence to this value is observed after 5 cycles, in concordance with results shown in the inset of Fig. 4, regardless of flow direction. The reduced χ^2 for the fitting to Eq. 2 was also calculated for all the cycles; the resulting value is about 1, indicating

an excellent adjustment of the power law function to every experimental curve.

Figure 6 presents the position of liquid front for a specified time (5 min) as a function of the cycle number, for all devices used. Data corresponding to the same device are connected by straight lines. It is observed that all paper strips follow the behavior described in Fig. 4. Fluid velocity increases during the first cycles and stabilizes in the last ones. It is also clear that the velocity difference between strips cut in fast (blue) and slow (red) flow directions. The velocity is about 10 ± 1 % higher in the fast direction, which is consistent with the axis ratio of the ellipse shown in Fig. 1b. In Fig. 6, the vertical dispersion for each cycle represents the variation between devices, which is approximately constant. The inter-strip variability is about 5 % for fast direction and 3 % for slow direction, and total variability is 7 %, as it was anticipated above.

3.2 Precise capillary flow

Up to this point, we have described how the filling dynamics changes when a paper strip undergoes a systematic wetting-drying process. In what follows, we discuss the possibility of achieving a high predictability of the filling dynamics. The fact is that the front position for one strip (at a given time) can be predicted by using the data of the previous filling. As inferred from results in Fig. 6, this goal can be accomplished by using data of the same strip only or, better, by using data from all strips. The position in the cycle $k+1$ can be estimated directly as the position in the cycle k for the same strip. The relative error e for this predictor is:

$$e = \frac{l_{k+1} - l_k}{l_{k+1}} \tag{3}$$

where l_i is the position extracted from Fig. 6 for one strip in the cycle i. Results for the six devices are presented in Fig. 7, including the associated standard deviation (bars). It can be observed that the cyclic process stabilizes the capillary filling. The position differences between subsequent cycles decrease with cycle number, and only four wetting–drying cycles are required to achieve a repeatability smaller than 2 %.

As mentioned above, the predictability can be improved if one employs data from other strips as a calibration. The behavior observed in Figs. 6 and 7 hints that the filling dynamics is the result of the combination of an intrinsic property of each strip and an effect produced by the wetting-drying process. This idea emerges from the fact that curves in Fig. 6 are conformal, i.e., the fastest strip in the first filling is the fastest strip in all cycles. Therefore, the effect of the kth drying process can be considered as a correction term $\Delta l(k)$ that, added to l_k, allows to predict l_{k+1}.

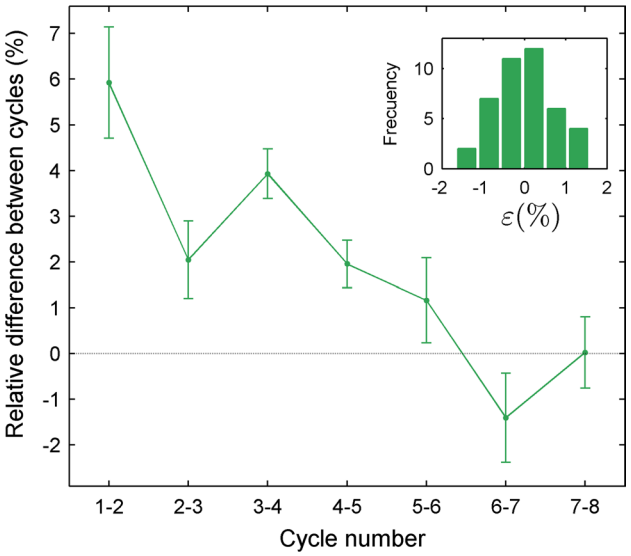

Fig. 7 Relative difference between the position at 5 min for consecutive cycles (Eq. 3). *Dots* represent the mean value for *six strips* and *bars* represent the standard deviation. The *inset* presents an histogram of relative error ε (Eq. 4) for all the cycles

The term $\Delta l(k)$ can be estimated by the mean value of $l_{k+1} - l_k$ for all strips. The relative error ε for this new predictor is:

$$\varepsilon = \frac{l_{k+1} - (l_k + \Delta l(k))}{l_{k+1}} \tag{4}$$

This error is approximately equal to the bars in Fig. 7. For example, the correction term between cycles 1 and 2 is estimated in $\Delta l(1) = 2.0$ mm (5.9 %). The error calculated with Eq. 4 is about 1.2 %, in accordance with the first bar in Fig. 7. A histogram of the errors ε for all cycles and all devices is presented in the inset of Fig. 7. A normal distribution is observed, which supports the proposal.

The whole method involving about 5 cycles allows one to achieve a relative error less than 0.8 %, meaning $\sim$350 µm in distance, which is comparable to the limit detection of our experimental setup. However, it is worth to remark that doing just one cycle results in a relative error still low (1.2 %).

Additional experiments (reported in the supplementary material) were made to corroborate these results and to test the stability during storage at normal conditions. It is found that the predictability of filling times holds for a relatively long time. The same strips were tested after being stored under normal (lab) conditions of humidity and temperature for two months. This suggests that the proposed protocol can be part of the device manufacturing process.

All experiments performed with chromatography paper were repeated using filter paper. The overall results are essentially the same, as shown in the supplementary material.

3.3 Paper-based viscometry

Here we use stabilized strips to perform precise viscometry on paper as one of the potential applications of well-predictable capillary flows. Imbibition experiments with glycerol and sucrose solutions were carried out on papers strips, which were previously stabilized by 5 wetting–drying cycles, as described above. Results are shown in Fig. 8, where $((l_5 + \Delta l(5))/l_6)^2 = (1 - \varepsilon)^2$, after Eq. 4 for a fixed imbibition time of 5 min, is plotted against tabulated viscosity data for different concentrations (Swindells et al. 1958). Note that $l_5 + \Delta l(5)$ is the predictor of the imbibition position of water at cycle 6, while l_6 is the measured imbibition position reached by solution at cycle 6. Besides, the ratio $(l_{\text{water}}/l_{\text{solution}})^2 = \mu_{\text{water}}/\mu_{\text{solution}}$, taking into account that d in Eq. 1 is inversely proportional to the fluid viscosity μ (Elizalde et al. 2015), and considering that surface tension is not significantly affected by the solute (Fassenden 1928). A remarkably good data correlation is observed in Fig. 8. Values were fitted with linear equation $y = m \cdot x$ with slope $m = 1.142 \pm 0.004\,\text{cP}^{-1}$ and correlation coefficient $R^2 = 0.9998$. Data points are overlapped in Fig. 8, indicating the high repeatability of the measured values. The small uncertainty obtained in the slope m (0.3 %) is a measure of the ultimate precision that can be attained with the procedure proposed here. As mentioned above, the wetting–drying cycles performed beforehand entail a precision of 0.8 %. The inaccuracy of the viscosity determination results from both contributions, which yields an overall error of about 1 %. Thus one may conclude that high-precision paper-based viscometry is achievable.

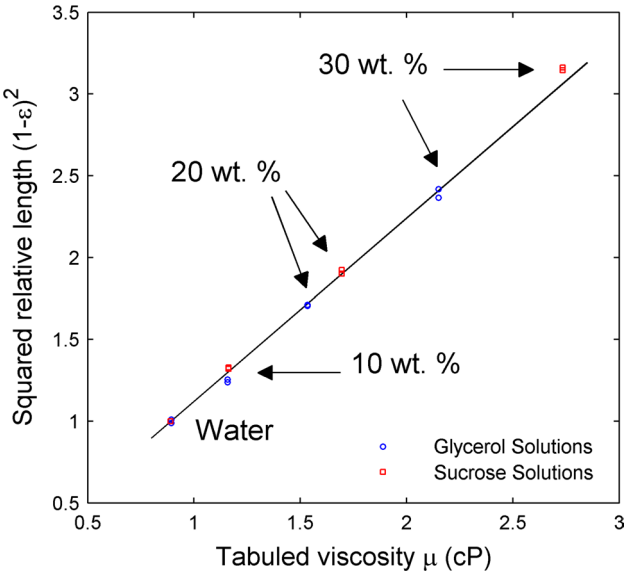

Fig. 8 Squared relative length from Eq. 4 as a function of tabulated viscosity values at 25 °C for glycerol (*blue circles*) and sucrose solutions (*red squares*). *Symbols* are experimental values (two trials for each concentration), and the continuous line is the linear fitting (color figure online)

4 Concluding remarks

In summary, this work describes the meticulous experimental analysis carried out to improve the precision and predictability of capillary imbibition in pure cellulose paper and, as a relevant outcome, proposes a precise paper-based viscometer. Some final remarks are outlined in this closing section.

Firstly, it must be pointed out that fixing the paper over a rigid substrate (hydrophobic double-sided tape was used for the purpose) is essential to maintain the material integrity while systematic wetting–drying cycles are performed. Besides, pernicious factors like evaporation and temperature gradients were carefully avoided in the experiments. Under the circumstances, one may conclude that the observed trends in the imbibitions dynamics are due to changes in the inner structure of the porous media, notably fibers reordering that influence the hydrodynamic resistance and washing of chemicals that affect capillary forces (Alava et al. 2004). These physicochemical aspects definitely deserve further research and are out of the scope of the present work.

Finally, it is worth to remark that the procedure described here enables a quantitative assessment of filling dynamics with uncertainties lower than 0.8 % if at least five cycles are made, or around 1.2 % when just one cycle is performed. This possibility would contribute to develop paper-based microfluidic devices with a new level of precision and hence to improve the sensibility and repeatability of μPADs. As a practical implementation, we have demonstrated that the viscosity of glycerol and sucrose solutions measured on stabilized paper strips has high correlation with tabulated data ($R^2 = 0.9998$).

Acknowledgments The authors thank the financial support received from the Consejo Nacional de Investigaciones Científicas y Técnicas (CONICET) and the Universidad Nacional del Litoral (UNL), Argentina.

References

Alava M, Dube M, Rost M (2004) Imbibition in disordered media. Adv Phys 53(2):83–175. doi:10.1080/00018730410001687363

Berli CLA, Urteaga R (2014) Asymmetric capillary filling of non-newtonian power law fluids. Microfluid Nanofluidics 17(6):1079–1084. doi:10.1007/s10404-014-1388-9

Bohm A, Carstens F, Trieb C, Schabel S, Biesalski M (2014) Engineering microfluidic papers: effect of fiber source and paper sheet properties on capillary-driven fluid flow. Microfluid Nanofluidics 16(5):789–799. doi:10.1007/s10404-013-1324-

Cai J, Yu B, Zou M, Luo L (2010) Fractal characterization of spontaneous co-current imbibition in porous media. Energy Fuels 24(3):1860–1867. doi:10.1021/ef901413p

Cate DM, Dungchai W, Cunningham JC, Volckens J, Henry CS (2013) Simple, distance-based measurement for paper analytical devices. Lab Chip 13:2397–2404. doi:10.1039/C3LC50072A

Cate DM, Adkins JA, Mettakoonpitak J, Henry CS (2015) Recent developments in paper-based microfluidic devices. Anal Chem 87(1):19–41. doi:10.1021/ac503968p

Connelly JT, Rolland JP, Whitesides GM (2015) paper machine for molecular diagnostics. Anal Chem 87(15):7595–7601. doi:10.1021/acs.analchem.5b00411

Elizalde E, Urteaga R, Berli CLA (2015) Rational design of capillary-driven flows for paper-based microfluidics. Lab Chip 15:2173–2180. doi:10.1039/C4LC01487A

Fassenden RW (1928) The viscosity and surface tension of dispersions of sucrose, lactose, skim milk powder, and butterfat. http://scholarworks.umass.edu/theses/1503/

Hong S, Kim W (2015) Dynamics of water imbibition through paper channels with wax boundaries. Microfluid Nanofluidics 19(4):845–853. doi:10.1007/s10404-015-1611-3

Jahanshahi-Anbuhi S, Henry A, Leung V, Sicard C, Pennings K, Pelton R, Brennan JD, Filipe CD (2014) Paper-based microfluidics with an erodible polymeric bridge giving controlled release and timed flow shutoff. Lab Chip 14(1):229–236

Joung YS, Figliuzzi BM, Buie CR (2014) Design of capillary flows with functionally graded porous titanium oxide films fabricated by anodization instability. J Colloid Interface Sci 423:143–150. doi:10.1016/j.jcis.2014.02.032

Lewis GG, Robbins JS, Phillips ST (2013) Point-of-care assay platform for quantifying active enzymes to femtomolar levels using measurements of time as the readout. Anal Chem 85(21):10432–10439. doi:10.1021/ac402415v

Li H, Han D, Pauletti G, Steckl A (2014) Blood coagulation screening using a paper-based microfluidic lateral flow device. Lab Chip 14(20):4035–4041

Liu Z, Hu J, Zhao Y, Qu Z, Xu F (2015) Experimental and numerical studies on liquid wicking into filter papers for paper-based diagnostics. Appl Therm Eng 88: 280–287. 10.1016/j.applthermaleng.2014.09.057, http://www.sciencedirect.com/science/article/pii/S1359431114008291

Lucas R (1918) Ueber das zeitgesetz des kapillaren aufstiegs von flüssigkeiten. Colloid Polym Sci 23(1):15–22

Martinez AW, Phillips ST, Whitesides GM, Carrilho E (2010) Diagnostics for the developing world: microfluidic paper-based analytical devices. Anal Chem 82(1):3–10. doi:10.1021/ac9013989

Masoodi R, Pillai KM (2010) Darcy's law-based model for wicking in paper-like swelling porous media. AIChE J 56(9):2257–2267

Noh H, Phillips ST (2010a) Fluidic timers for time-dependent, point-of-care assays on paper. Anal Chem 82(19):8071–8078

Noh H, Phillips ST (2010b) Metering the capillary-driven flow of fluids in paper-based microfluidic devices. Anal Chem 82(10):4181–4187

Press WH, Teukolsky SA, Vetterling WT, Flannery BP (2007) Numerical recipes: the art of scientific computing, 3rd edn. Cambridge University Press, New York

Shou D, Ye L, Fan J, Fu K, Mei M, Wang H, Chen Q (2014) Geometry-induced asymmetric capillary flow. Langmuir 30(19):5448–5454. doi:10.1021/la500479e

Shou D, Fan J (2015) The fastest capillary penetration of power-law fluids. Chem Eng Sci 137: 583–589. 10.1016/j.ces.2015.07.009, http://www.sciencedirect.com/science/article/pii/S0009250915004947

Songok J, Salminen P, Toivakka M (2014) Temperature effects on dynamic water absorption into paper. J Colloid Interface Sci 418:373–377. doi:10.1016/j.jcis.2013.12.017

Songok J, Toivakka M (2016) Controlling capillary-driven surface flow on a paper-based microfluidic channel. Microfluid Nanofluidics 20(4):1–9

Swindells JF, Snyder CF, R.C.H, Golden PE (1958) Viscosities of sucrose solutions at various temperatures: Tables of recalculated values. Technical report, National Bureau of Standards

Wang X, Hagen JA, Papautsky I (2013) Paper pump for passive and programmable transport. Biomicrofluidics 7(1):014,107. doi:10.1063/1.4790819

Washburn EW (1921) The dynamics of capillary flow. Phys Rev 17(3):273

Xiao J, Stone HA, Attinger D (2012) Source-like solution for radial imbibition into a homogeneous semi-infinite porous medium. Langmuir 28(9):4208–4212. doi:10.1021/la204474f

Yetisen AK, Akram MS, Lowe CR (2013) Paper-based microfluidic point-of-care diagnostic devices. Lab Chip 13(12):2210. doi:10.1039/c3lc50169h